

1995/08/163
350305

109

ROLE OF DIELECTRIC CONSTANT IN ELECTROHYDRODYNAMICS OF CONDUCTING FLUIDS

Percy H. Rhodes and Robert S. Snyder
National Aeronautics and Space Administration
George C. Marshall Space Flight Center
Huntsville, Alabama 35812

Glyn O. Roberts
Roberts Associates, Inc.
11794 Great Owl Circle
Reston, Virginia 22094

ABSTRACT

Electrohydrodynamic sample distortion during continuous flow electrophoresis is an experiment to be conducted during the second International Microgravity Laboratory (IML-2) in July 1994. The specific objective of this experiment is the distortion caused by the difference in dielectric constant between the sample and surrounding buffer. Although the role of sample conductivity in electrohydrodynamic has been the subject of both flight and ground experiments, the separate role of dielectric constant, independent of sample conductivity, has not been measured. This paper describes some of the laboratory research and model development that will support the flight experiment on IML-2.

INTRODUCTION

The role of electric conductivity tends to overshadow the effect of dielectric constant in many electrohydrodynamic (EHD) experiments. Melcher and Taylor [7] make the following observations. "Electrostatic effects in fluids are known for their vagaries; often they are so extremely dependent on electrical conduction that investigators are discouraged from carefully analytical models and simple experiments." Our early experiments [5] studying the EHD deformations of cylindrical streams readily showed the conductivity effect but the dielectric constant effect was not discernible. We have modified our flow chamber and enhanced our method of observation and can now see an unequivocal dielectric constant effect which is in agreement with the theory given in [5].

In this paper we first give a brief description of the physics of charge buildup at the interface of an immersed spherical drop or flowing cylindrical sample stream and then show how these charge distributions lead to interface distortions and accompanying viscous flows which constitute EHD. We next review theory and experiment describing the deformation of spherical drops of one fluid in another and show that there is no significant dielectric constant effect on the mode of deformation. We review our work [5] describing the deformation of a cylindrical stream of one fluid flowing in a carrier buffer and compare the deformation equations to those of the spherical drops. Finally, we show a definite dielectric constant effect in our case for a cylindrical sample stream of polystyrene latex as a function of the frequency of the excitation field.

INDUCED CHARGE FOR A DROP OR CYLINDER

In this study we consider the EHD flows associated with spherical drops or circular cylinders of an inside fluid in a surrounding outside fluid. We review theoretical and experimental work done by others and ourselves, and attempt to explain their structure and sign physically. Figure 1 shows the spherical or cylindrical geometry, and adds electrodes to indicate an imposed field direction from left to right.

It can be shown that there is no induced charge in the homogeneous regions. Charge is induced only at the interface.

From charge continuity, Ohm's law, and Maxwell's equations, the surface charge is

$$4\pi q_s = j_n(K_o / \sigma_o - K_i / \sigma_i), \tag{1}$$

where K and σ are the dielectric constant and electric conductivity, respectively. The current density normal to the interface is j_n . The subscript i denotes the region inside the drop or stream while o denotes the surrounding region (outside). Defining the conductivity and dielectric constant ratios as

$$R = \sigma_i / \sigma_o, \tag{2}$$

$$S = K_i / K_o, \tag{3}$$

Equation (1) can be rewritten as

$$4\pi q_s = (R - S)j_n K_o / \sigma_i. \tag{4}$$

The current in Fig. 1 is from left to right. So on the right half of the interface the outward normal current j_n is positive, and the interface charge density q_s has the same sign as $(R-S)$. Thus q_s is negative on the right in Fig. 1a, where

$$R < 1 < S,$$

and positive on the right in Fig. 1b, where

$$R > 1 > S.$$

On the left half of the interfaces in Fig. 1, the outward normal current j_n is negative, and the induced charge in Fig. 1a and 1b has the opposite sign, as shown.

FLOW CALCULATION

Once the electric field solution and the associated induced charge density have been found, the corresponding flow is determined by solving the Navier-Stokes equations, with the electric forces included. The electric forces can be equivalently expressed either in terms of the Maxwell stress tensor (convenient for interface boundary conditions) or as the sum of the electric forces on the charge density and on the dipole distribution associated with the dielectric constant.

On the scales of interest, fluid momentum can normally be neglected. The flow is therefore a balance between the electric forces, viscosity, and pressure gradients, with the incompressibility condition. Interface surface tension must be included in determining the change of shape of drops.

We have chosen not to give details in this review. But inspection of Fig. 1a suggests that with the electric field from left to right, the electric forces pull the positive and negative charges towards each other, flattening the circle normal to the electric field. And in Fig. 1b, the electric forces on the positive and negative surface charge distributions pull them apart, tending to elongate the circle toward the electrodes. This is confirmed by the detailed computations for the drop and cylindrical geometries. For the two special cases shown in Fig. 1a and 1b, the inclusion of the dipole electric forces does not change the solution qualitatively.

On the other hand, when R and S are either both greater than unity or both less than unity, dielectric forces can change the qualitative picture. In particular, Equation (4) shows that for $R = S$ there is no induced charge on the surface. But the detailed calculations show non zero EHD flow in this case, except in the trivial case $R = S = 1$.

THEORY OF DROP DEFORMATION

This early work on EHD flows was concerned with drop deformation, and used immiscible fluids. A neutrally buoyant spherical drop of one fluid in the other was distorted against surface tension by the application of a uniform AC field, and the shape distortion was measured and compared with theory.

The theory for conducting fluids was given by Taylor [1], and is known as Taylor's "leaky dielectric" model. Taylor obtains the drop deformation (defined as the difference of the drop axis lengths (diameters) divided by their sum, and positive for a prolate spheroid) in the form

$$\Omega = (9/64\pi)(K_o a E^2 / \gamma) \Phi / (2+R)^2. \quad (5)$$

In this equation, γ is the surface tension, a the drop radius, E the imposed root mean square electric field, and the dimensionless discriminating function is

$$\Phi = 1 + R^2 - 2S + N(R - S). \quad (6)$$

Here

$$N = (6M + 9) / (5M + 5), \quad (7)$$

$$M = \mu_i / \mu_o, \quad (8)$$

and μ_i and μ_o are the inner and outer viscosities. Thus N decreases from 1.8 to 1.2 as the viscosity ratio M increases from zero to infinity, and is 1.5 when M is 1. Using these values for N , Equation (6) becomes

$$\text{for } M = 0, \quad \Phi = R^2 + 1.8R + 1 - 3.8S, \quad (9)$$

$$\text{and for } M \rightarrow \infty, \quad \Phi = R^2 + 1.2R + 1 - 3.2S. \quad (10)$$

Note that Taylor used the reciprocal S definition to our Equation (3), we have therefore changed his results appropriately to obtain our Equations (5) and (6). If Φ is positive, the spherical drop is elongated in the electric field direction, into a prolate spheroid. If Φ is negative, the drop is flattened normal to the electric field direction, into an oblate spheroid.

DROP DEFORMATION EXPERIMENTS

Many reported EHD studies have measured the electrical deformation of spherical drops, using various combinations of immiscible fluids. In this review, we emphasize the significance of dielectric constant effects. In our view, none of these reported results unequivocally demonstrated such effects, since in all cases the sign of the discriminating function (6) was the same as if the dielectric constant ratio had been 1. Note that from Equation (6) the critical value of the dielectric constant ratio S is

$$(1 + NR + R^2)/(2 + N).$$

Figure 3 shows the critical S value as a function of R over the range of M . For smaller S values, the drop becomes prolate, elongated in the field direction. For larger S values it becomes oblate, flattened normal to the field. An unequivocal demonstration of a dielectric constant effect in EHD requires a sign change in the drop distortion. For $R < 1$ this requires that S is less than the critical value, while for $R > 1$ it requires that S is greater than the critical value. Otherwise we can say that the sign of the discriminating function is "controlled" by R .

In these admittedly difficult experiments, measuring and controlling the conductivities and controlling the interface surface tension are often the hardest problems. In Equation (5), $\Phi/(2 + R)^2$ simplifies to 1 for large conductivity ratio R and to $(1 - 2S - NS)/4$ for small R . Intermediate R values have been avoided in the reported results, apparently due to the conductivity difficulties. For large R , the critical S value is very large, while for R close to zero, it is just $1/(2 + N)$, or about 0.3, as Fig. 3 shows.

Allan and Mason [2] reported drop deformation experiments with 13 different combinations of fluids. In all cases the observed deformation correlated with Φ , and was also that expected for the measured conductivity ratio R . The experimental R values ranged up from 15, or down from 1/15. In terms of Equations (5) and (6), these experiments did not demonstrate a dielectric effect; the results were qualitatively the same as if S had been unity.

Torza, Cox, and Mason [3] reported 22 fluid combinations, which were all controlled by the conductivity ratio R . Similarly, Vizika and Saville [4] reported 11 fluid combinations; also controlled by R . In the small R cases in [2] through [4], the smallest S value was 0.44, or substantially above the critical value of $1/(2 + N)$. A smaller value would have provided an unequivocal demonstration of dielectric constant effects in EHD.

DIELECTRIC CONSTANT OF AQUEOUS SUSPENSIONS

Clays and aqueous suspensions can be polarized, and act as homogeneous fluids with very high dielectric constants. This phenomenon is associated with the electrochemical charge double layer on each particle. As the particle and its surrounding charge cloud respond to the external field, and undergo electroosmosis, they also become a dipole. The higher the frequency for AC, the less time there is for the charge to move. Thus K decreases with increasing frequency, as shown in Fig. 2.

The dielectric constant of a suspension is measured experimentally by using an accurate bridge technique to determine the complex resistance of an electrolytic cell, as a function of frequency. This is not easy, and comparisons with theory have been mixed.

Over the last several years we have studied the deformation of cylindrical sample streams consisting of dispersions of polystyrene latex (PSL) microspheres [5,6]. The sample is drawn into a fine filament as it is injected into a flowing carrier buffer. The major difference between our system and the immiscible drop system discussed previously is the absence of surface tension in our case. The application of a uniform electric field to the cylindrical sample filament will distort the sample stream into a ribbon. The orientation of the ribbon depends on the ratios of dielectric constant and electrical conductivity between the buffer and sample. These distortions are the result of EHD flows in both the sample and buffer. The leaky dielectric model of Taylor is again used to determine the degree and orientation of the sample stream distortion. For a circular sample stream of properties shown in Fig. 1, we showed [5] that the radial EHD velocity u at the interface is given by

$$u = FD \cos 2\theta, \tag{11}$$

where the amplitude function is

$$F = \frac{aE^2 K_0}{12\pi(\mu_i + \mu_o)(R + 1)^2} \tag{12}$$

and the discriminating function is

$$D = R^2 + R + 1 - 3S. \tag{13}$$

Here θ is the polar coordinate angle measured from the electric field direction. Note that the angular dependence $\cos 2\theta$ implies distortion of the circular sample section to an ellipse. From qualitative theoretical study [5] and from all our observations, this distortion continues until the sample becomes a flattened ribbon, either aligned with the field or perpendicular to it. Note the

similarity between this discrimination function D given by Equation (13), and the earlier function Φ for drop deformation, given by Equation (6). Both are different from the approximate discriminating function (R - S) suggested by Equation (4) and by the qualitative approximation of considering only the forces on free charges in computing the flow. To directly compare the discriminating function for liquid drops Φ to the discriminating function D for liquid streams, note the similarities between Equations (9), (10), and (13).

PSL SAMPLE STREAM DISTORTION EXPERIMENTS

In our experiments with sample stream distortion, we could vary the conductivity of both fluids. But we could not at first find a dielectric constant effect. Part of the problem was the low sensitivity of our early system, which was an electrophoresis type chamber limited to 30 V/cm. In addition, we were expecting K values from 200 to 1000 and higher, based on published literature for PSL suspensions. In fact, it appears that our samples were much closer to the water and buffer K value of 80. We improved the sensitivity of our method by using a small square chamber, allowing fields up to 300 V/cm, and by observing the distorted stream using a microscope system with a CCD camera and video monitor, at 62.5 magnification. Physically, the sample stream distortion was increased by a factor of 100, because of the E^2 dependence shown in Equation (12). Thus, our sensitivity improved by a factor of 6,250. With this system we have been able to demonstrate the EHD effects of the variations of dielectric constant with frequency, as shown in Fig. 2. These demonstrations are now repeatable.

Figure 4 shows eight views of steady EHD flows in our apparatus. The eight percent sample is injected through the circular nozzle just visible on the right. The transparent buffer, with matched conductivity, also enters the chamber from the right. In Fig. 4a there is no applied field, and the PSL passes along the chamber as a circular cylinder of constant diameter. The changes in cylinder diameter near the nozzle are associated with the nozzle drag on the buffer and PSL flow and with the viscous adjustment to a more uniform downstream flow profile. In the rest of Fig. 4 there is a fixed external AC electric field in the viewing direction; only the frequency is varied. The internal dimension for the square chamber is .5 cm, which gives a voltage gradient of 200 volts/cm throughout the run. No changes are made in the buffer or sample fluids or flow rates. In Fig. 4b, at 100,000 Hz, R and S are 1, and there is no EHD flow. At lower frequencies S increases, according to Fig. 2 and Equation (3). This makes the discriminant (13) increasingly negative, so that the circular sample stream is progressively flattened into a ribbon normal to the field, as it passes downstream to the left. For the lowest frequency of 28 Hz, this flattening is very rapid.

This series of photographs vividly shows the dielectric constant effect on EHD, and its variation with frequency, for a PSL sample filament. It also suggests a method for the measurement of dielectric constant. The stream at each frequency can be brought to zero deformation by adjustment of the conductivity ratio R . This value of R can then be used in Equation (13) (with $D=0$) to calculate S and, hence, K_j . The PSL particles were made using a recipe without emulsifier, and each polymer (styrene) chain is terminated with a sulfate and end group at each end. The sample was sonicated and centrifuged, and then placed in R-1 (phosphate) buffer to form the sample stock. The final conductivity was adjusted using distilled water. The R-1 buffer used had a pH of 7.08.

CONCLUSIONS

We believe that the sample stream distortions which are shown in Fig. 4 are the first experimental evidence of the dielectric constant effect in conducting fluids to appear in the literature. We are continuing work on our miniature flow chamber to improve the uniformity of the electric field while still maintaining clear observation of the sample stream when viewed parallel to the field. We will now quantify a selection of PSL with respect to debye length (κ^{-1}), zeta potential ζ , and particle radius a . The dielectric constant of this selection can then be determined as a function of frequency ν by the method previously described. This data will then be described by a Cole-Cole relaxation frequency distribution which can be compared to the standard model of Delacy and White [8] and to dielectric spectroscopy measurements of Myers and Saville [9].

REFERENCES

1. Taylor, G.I. 1966 Studies in electrohydrodynamics. I. The circulation produced in drop by an electric field. Proc. R. Soc. London 291, 159-166.
2. Allan, R.S., & Mason, S.G. 1962 Particle behaviour in shear and electric fields. I. Deformation and burst of fluid drops. Proc. R. Soc. London A 267, 45-61.
3. Torza, S., Cox, R.G. & Mason, S.G. 1971 Electrohydrodynamic deformation and burst of liquid drops. Phil. Trans. R. Soc. London 269, 259-319.
4. Vizika, O. & Saville, D.A. 1992 The electrohydrodynamic deformation of drops suspended in liquids in steady and oscillatory electric fields. J. Fluid Mech. 239, 1-21.
5. Rhodes, P.H., Snyder, R.S., & Roberts, G.O. 1989 Electrohydrodynamic distortion of sample streams in continuous flow electrophoresis. J. Colloid Interface Sci. 129, 78-90.
6. Rhodes, P.H., Snyder, R.S., Roberts, G.O. & Baygents, J.C. 1991 Electrohydrodynamic effects in continuous flow electrophoresis. Applied and Theoretical Electrophoresis 2/3, 87-91.
7. Melcher, J.R. & Taylor, G.I. 1969 Electrodynamics: a review of the role of interfacial shear stresses. Ann. Rev. Fluid Mech. 1, 111-146.

8. Delacey, E.B. & White L.R. 1981 Dielectric response and conductivity of dilute suspensions of colloidal particles. J. Chem. Soc. Faraday Trans. 2, 77, 2007-2039.
9. Myers, D.F. & Saville, D.A. 1989 Dielectric Spectroscopy of Colloidal Suspensions: II. Comparisons Between Experiment and Theory. J. Colloid Interface Sci. 131, 461-470.

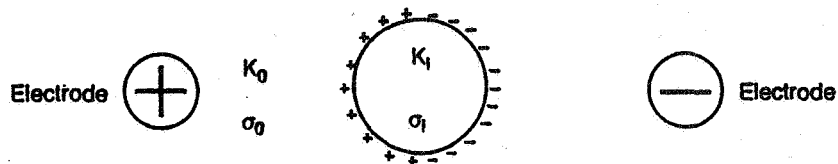


Fig. 1a. Charge distribution for $K_1 > K_0$ and $\sigma_1 < \sigma_0$ producing distortion normal to the field (oblate)

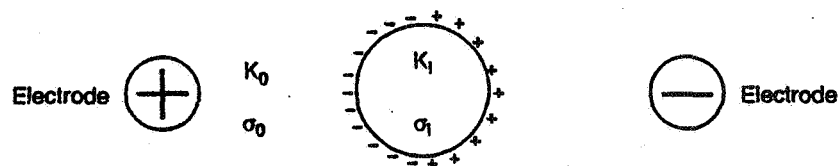


Fig. 1b. Charge distribution for $K_1 < K_0$ and $\sigma_1 > \sigma_0$ producing distortion parallel to the field (prolate)

Figure 1. Charge Distribution at the Interface and Resulting EHD Flows

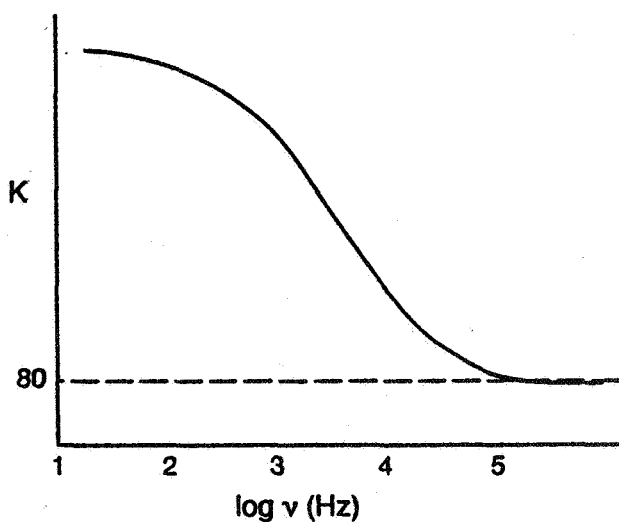


Figure 2. Variation of Dielectric Constant with Frequency ν for PSL Suspensions

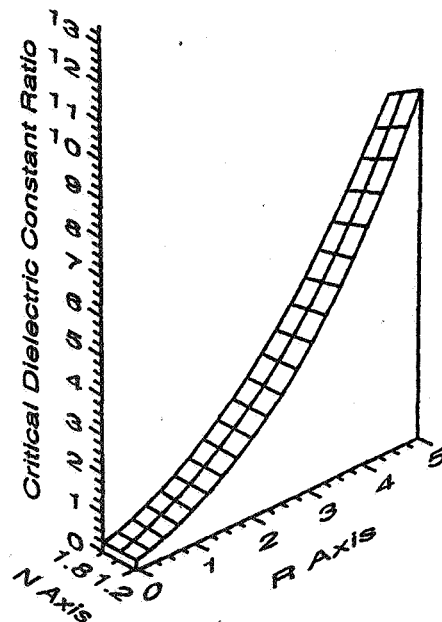
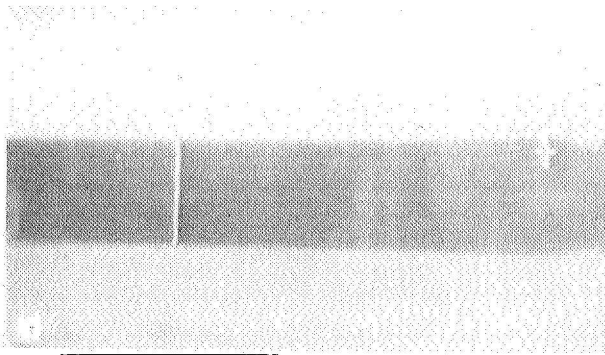
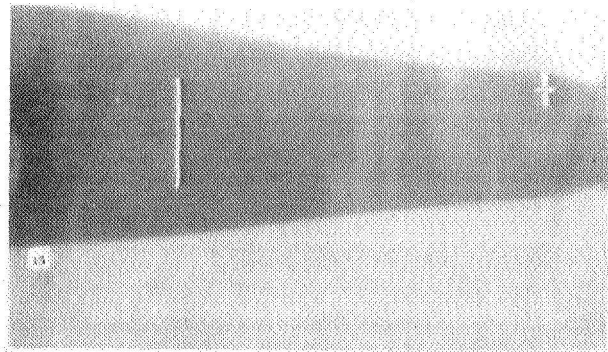


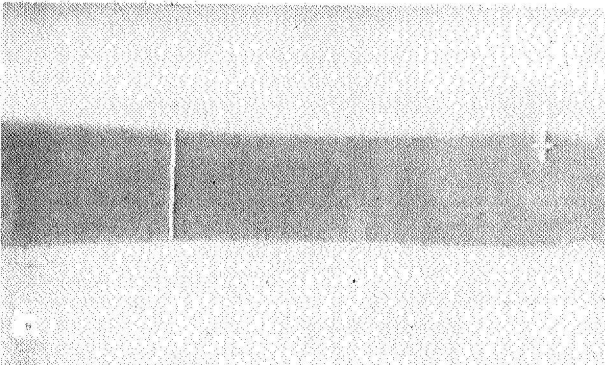
Figure 3. Relationship of Critical S to R



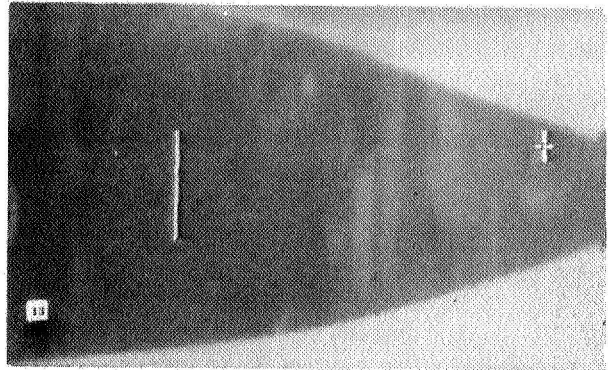
4a Zero Electric Field



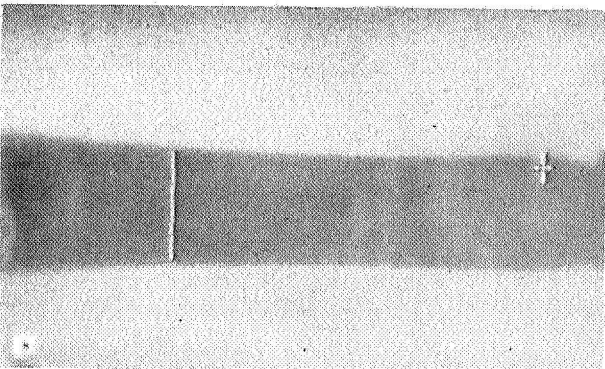
4e. 100 Volts RMS. 5,000 Hz Frequency



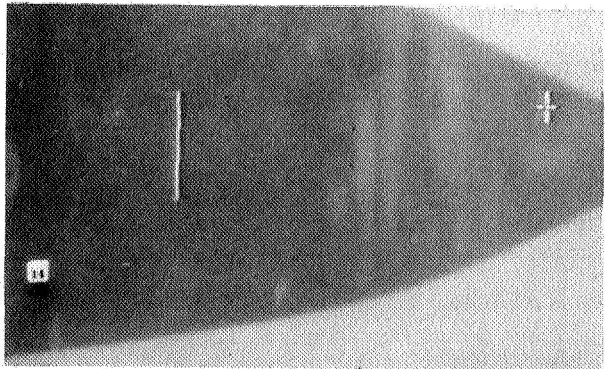
4b. 100 Volts RMS. 100,000 Hz Frequency



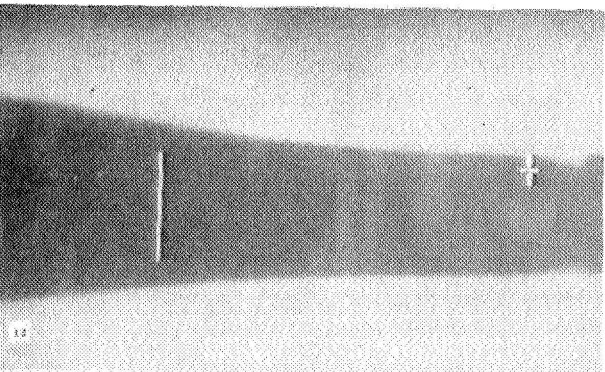
4f. 100 Volts RMS. 1,000 Hz Frequency



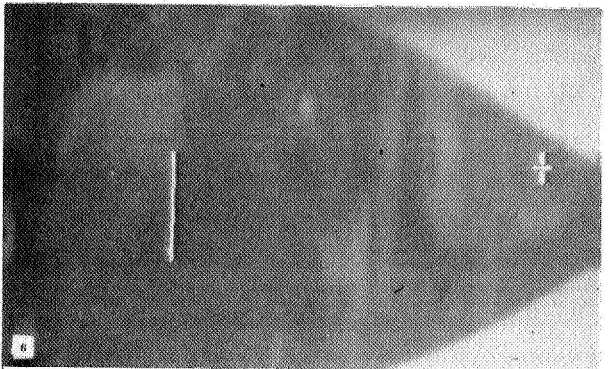
4c. 100 Volts RMS. 50,000 Hz Frequency



4g. 100 Volts RMS. 100 Hz Frequency



4d. 100 Volts RMS. 10,000 Hz Frequency



4h. 100 Volts RMS. 28 Hz Frequency

Fig 4 Sample stream distortions viewed parallel to the AC electric fields at varying frequency, using an 8% PSL sample.